International Journal of Mass Spectrometry 316–318 (2012) iv–xiii

Contents lists available at ScienceDirect

International Journal of Mass Spectrometry

journal homepage: www.elsevier.com/locate/ijms

Contents

Foreword

1–1

Foreword

Béla Paizs and Veronica M. Bierbaum

2–4

Personal Foreword-Alexander George Harrison

Robert K. Boyd and Raymond E. March

5–5

Curriculum Vitae-Alexander George Harrison

Regular Papers

6–11

Biomolecular condensation via ultraviolet excitation in vacuo

Sunyoung Lee, Ryan R. Julian, Stephen J. Valentine, James P. Reilly, David E. Clemmer

► We demonstrate the gas-phase synthesis of several different biomolecules using 157 nm vacuum ultraviolet irradiation (VUV) of charge-bound dimers. ► Several examples include the linear coupling of amino acid chains, intermolecular cross-linking, and glycosidic bond formation. ► Simple mechanisms for each case are proposed.

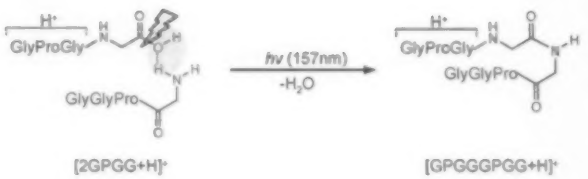

12–17

Competition between diketopiperazine and oxazolone formation in water loss products from protonated ArgGly and GlyArg

Shen Zou, Jos Oomens, Nick C. Polfer

► The water loss products from protonated ArgGly and GlyArg are investigated by infrared multiple photon dissociation spectroscopy and computational chemistry. ► While ArgGly exclusively yields diketopiperazine structures, a mixture of diketopiperazine and oxazolone structures are confirmed for GlyArg. ► Product structures due to nucleophilic attacks from the guanidine side chain can be excluded.

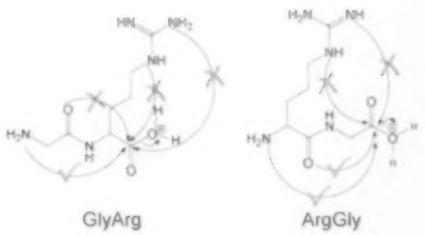

Elsevier B.V.
http://dx.doi.org/10.1016/S1387-3806(12)00148-0

International Journal of Mass Spectrometry 316–318 (2012) iv–xiii

Contents lists available at ScienceDirect

International Journal of Mass Spectrometry

journal homepage: www.elsevier.com/locate/ijms

Contents

Foreword

1–1

Foreword

Béla Paizs and Veronica M. Bierbaum

2–4

Personal Foreword-Alexander George Harrison

Robert K. Boyd and Raymond E. March

5–5

Curriculum Vitae-Alexander George Harrison

Regular Papers

6–11

Biomolecular condensation via ultraviolet excitation in vacuo

Sunyoung Lee, Ryan R. Julian, Stephen J. Valentine, James P. Reilly, David E. Clemmer

► We demonstrate the gas-phase synthesis of several different biomolecules using 157 nm vacuum ultraviolet irradiation (VUV) of charge-bound dimers. ► Several examples include the linear coupling of amino acid chains, intermolecular cross-linking, and glycosidic bond formation. ► Simple mechanisms for each case are proposed.

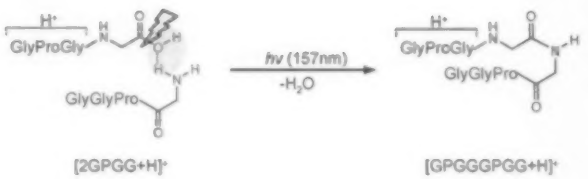

12–17

Competition between diketopiperazine and oxazolone formation in water loss products from protonated ArgGly and GlyArg

Shen Zou, Jos Oomens, Nick C. Polfer

► The water loss products from protonated ArgGly and GlyArg are investigated by infrared multiple photon dissociation spectroscopy and computational chemistry. ► While ArgGly exclusively yields diketopiperazine structures, a mixture of diketopiperazine and oxazolone structures are confirmed for GlyArg. ► Product structures due to nucleophilic attacks from the guanidine side chain can be excluded.

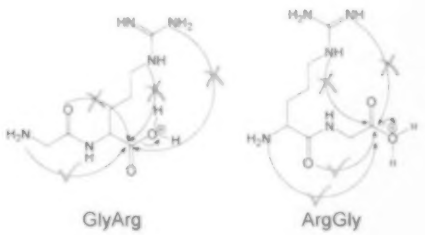

Elsevier B.V.
http://dx.doi.org/10.1016/S1387-3806(12)00148-0

18–22

The double hydrogen transfer in the 1-methoxy-2-propanol molecular ion: Loss of $CH_3CO^•$ by proton-transport catalysis

Karl J. Jobst, Nico M.M. Nibbering, Johan K. Terlouw

► Low-energy 1-methoxy-2-propanol ions lose $CH_3C{-}O^•$. ► Hydrogen-bridged radical cations (HBRCs) are predicted by theory to be key intermediates. ► A key step in the reaction involves proton-transport catalysis.

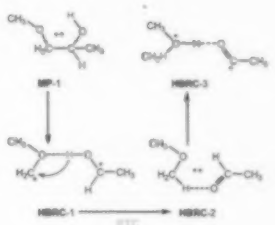

23–30

Bond activation in complexes of Pb(II) with 15 deprotonated amino acids: correlation with gas-phase acidity

Laura Banu, Voislav Blagojevic, Diethard K. Bohme

► Electrospray tandem mass spectrometry of gas-phase metal–dication complexes. ► Complexes of Pb^{2+} with 15 different deprotonated biological amino acids. ► Role of metal dication-induced bond activation in ion dissociation. ► Correlation of dissociation onset energies with amino acid gas-phase acidity.

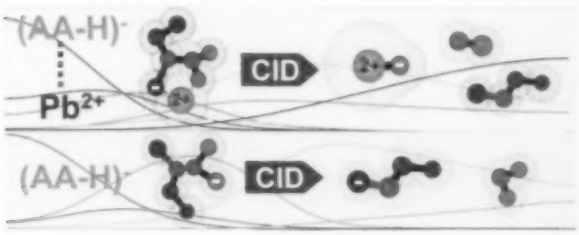

31–39

Investigating the relationship between the gas-phase conformations and dissociation energetics of peptide–saccharide complexes

Amanda N. Comeau, Justin B. Renaud, Gleb G. Mironov, Maxim V. Berezovski, Paul M. Mayer

► Link between dissociation energies and conformations of peptide–saccharide complexes. ► MM/MD structures correlated with ion mobility arrival time distributions. ► Isomeric saccharides exhibit distinct gas-phase conformations with FLEEL(V).

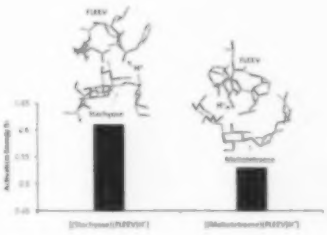

40–46

Dissociative protonation and fragmentation: Retro-Friedel–Crafts reactions of heterocyclic drug and metabolite molecules in mass spectrometry

Ya-Ping Tu

► We studied the electrospray mass spectrometry of tolmetin, naratriptan and lansoprazole, which are derivatives of pyrrole, indole and benzimidazole. ► Prominent fragmentation through deacylation, dealkylation, desulfoxidation and desulfonation was observed. ► Preferred protonation sites are determined for these heterocyclic drug and metabolite molecules. ► The major fragmentation is induced by protonation at the dissociative protonation site, which is not the preferred site for protonation.

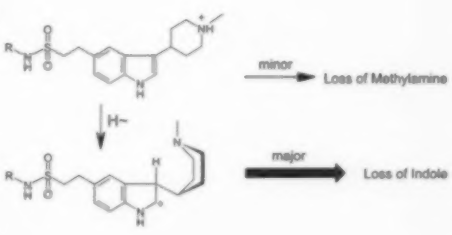

47–56

Gas-phase basicity and acidity of tryptophan

Vanessa Riffet, Sophie Bourcier, Guy Bouchoux

► Extensive exploration of conformational space of neutral, protonated and deprotonated tryptophan at the G4MP2 computational level. ► New clues for the interpretation of spectroscopic and mass spectrometry data concerning tryptophan. ► G4MP2 computation of gas phase acidity and basicity of tryptophan. ► Experimental determination of the gas phase basicity of tryptophan by the extended kinetic method.

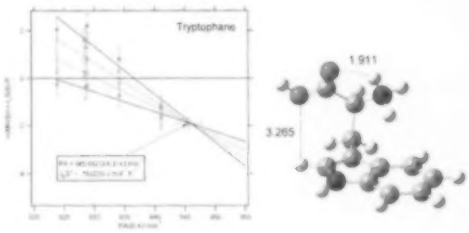

57–67

Protonation sites in peptide dications and cation-radicals containing β-amino acid residues

Christopher L. Moss, František Tureček

► Protonation in peptides containing β-amino acid residues occurs at amide O-atoms. ► $N–C_\alpha$ bond dissociations outcompete $N–C_\beta$ bond cleavages at β-amino acid residues. ► Hydrogen atom migrations between amide groups compete with $N–C_\alpha$ bond cleavage.

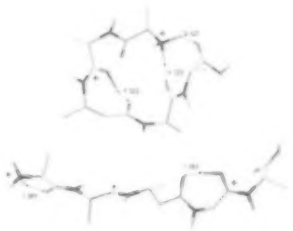

68–75

The gas-phase reactions of metal porphyrins with diazoacetate esters

Jamal T. Aldajaei, Scott Gronert

► Gas-phase reactions of metal porphyrins with diazoacetates to give carbenes. ► Fragmentation gives novel metal species including CH and C=C=O complexes. ► Computations indicate strong preference for bridging in metal carbenes. ► Bridging will have critical effect on activity of these cationic catalysts.

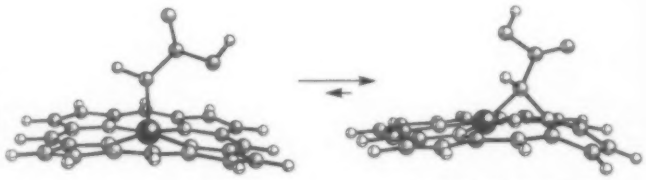

76–83

Reactions of nitrophenide and halonitrophenide ions with acrylonitrile and alkyl acrylates in the gas phase: The case of $[M-2]^-$ ion formation

Magdalena Zimnicka, Osamu Sekiguchi, Einar Uggerud, Witold Danikiewicz

► Nitrophenide ions react with α,β-unsaturated compounds via formation of β-adducts. ► Unstable β-adducts rearrange to derivatives of o-nitrosobenzylic anion ($[M-2]^-$). ► The mechanism involves an O-atom transfer via a six-membered intermediate. ► The formation of $[M-2]^-$ ions is characteristic of nitrophenide ions.

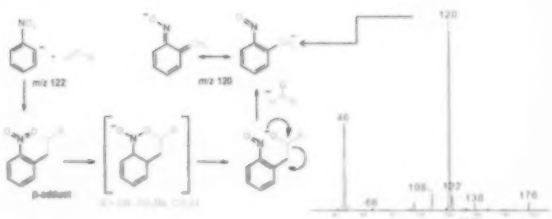

84–90

The role of lysine ε-amine group on the macrocyclization of *b* ions

A. Emin Atik, Guvenc Gorgulu, Talat Yalcin

► N-terminal acetylated model octapeptides containing lysine, glutamine or asparagine located at the N-terminal position 1 were studied to investigate the effect of ε-amine group on the macrocyclization of *b* ions. ► Lysine ε-amine group is involved in the *b*-type macrocyclization. ► Position of lysine residue in the N-terminal acetylated model octapeptides is important.

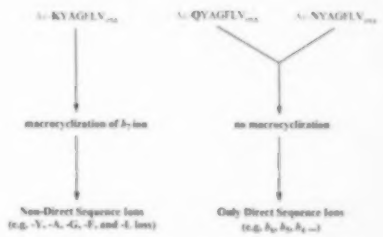

91–99

Gas-phase ion chemistry of the pesticide imidacloprid: Proton driven radical fragmentation of the nitro-guanidine functional group

William A. Donald, Micnael G. Leeming, Richard A.J. O'Hair

► Protonated imidacloprid, a small molecule pesticide, undergoes radical fragmentation upon collision induced dissociation. ► The proton is mobile and is tranferred between basic sites to trigger radical fragmentation of the nitroguanidine group. ► The nitroguanidine functional group acts as a "proton affinity switchable explosophore" that scavenges a proton and expels $NO_2^{\bullet}$. ► This functional group might be useful for generating radicals in protonated biomolecules using collision induced dissociation.

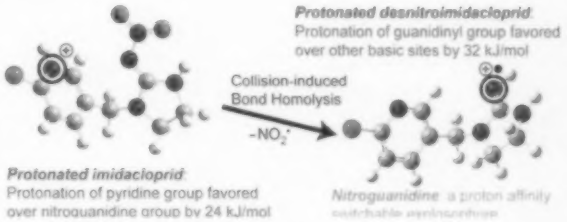
Protonated desnitroimidacloprid
Protonation of guanidinyl group favored over other basic sites by 32 kJ/mol
Collision-induced Bond Homolysis
$-NO_2^{\bullet}$
Protonated imidacloprid
Protonation of pyridine group favored over nitroguanidine group by 24 kJ/mol
Nitroguanidine a proton affinity

100–107

Evaluation of ion activation strategies and mechanisms for the gas-phase fragmentation of sulfoquinovosyldiacylglycerol lipids from *Rhodobacter sphaeroides*

Xi Zhang, Cassie J. Fhaner, Shelagh M. Ferguson-Miller, Gavin E. Reid

► The SQDG *m/z* 225 product ion provides the greatest sensitivity for lipid detection in triple quad. mass spectrometers. ► High res./accur. mass HCD-MS/MS is the most sensitive/specific strategy for SQDG lipid identification and characterization. ► High res./accur. mass MS/MS and H/D exchange facilitates elucidation of mechanisms for deprotonated lipid ion fragmentation.

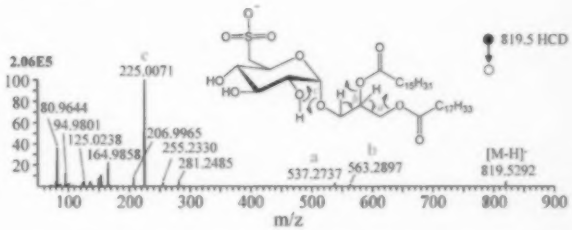

108–116

Investigation of peptide size, residue position, neighbor amino acid and side chain effect on macrocyclization of b_n (n = 5–7) ions

Cagdas Tasoglu, Guvenc Gorgulu, Talat Yalcin

► b_6 and b_7 ions have higher tendency of macrocyclization compared to b_5 ions with the exception of QYAGFLV-NH_2. ► No preferential cleavage order can be specified depending on nature of amino acid side chain. ► Selective ring opening depends on the size of *b* ions and the position of the amino acid residue. ► Neighbor amino acid has influenced the selective opening of macrocyclic b_6 ion.

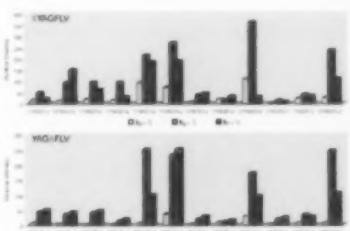

117–125

Structure, energetics and vibrational spectra of protonated chlortetracycline in the gas phase: An experimental and computational investigation

Blake E. Ziegler, Rick A. Marta, Sabrina M. Martens, Jonathan K. Martens, Terry B. McMahon

▶ IRMPD spectra of protonated chlortetracycline have been obtained. ▶ Electronic structure calculations of possible isomers and tautomers are presented. ▶ Computed vibrational spectra and experimental IRMPD spectra have been compared. ▶ Probable structure identification of protonated chlortetracycline has been made. ▶ Future experiments to aid in structural assignment have been proposed.

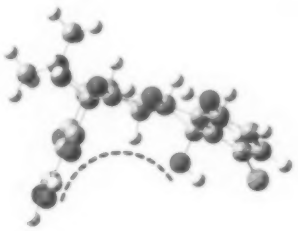

126–132

Gas-phase acidities of lysine homologues and proline analogs from the extended kinetic method

Ian K. Webb, Corbin E. Muetterties, Charlotte B. Platner, John C. Poutsma

▶ We determined ΔH_{acid} values for three lysine homologues and two proline analogs. ▶ We used the extended kinetic method and density functional theory calculations. ▶ The acidities of the three lysine homologues are the same within error. ▶ The acidities of the two proline analogs are the same within error.

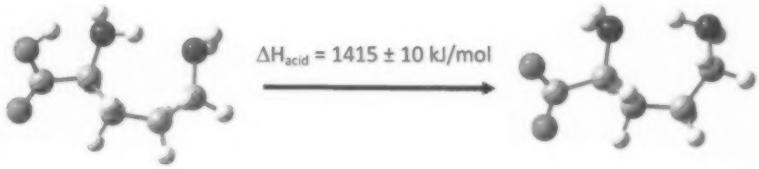

133–139

Gas-phase reactivity of sulfur-based radical ions of cysteine derivatives and small peptides

Sandra Osburn, Richard A.J. O'Hair, Victor Ryzhov

▶ Cysteine-based thiyl radical ions display typical sulfur radical reactivity in the gas phase. ▶ Reactivity is radical-based and is not affected by charge of the radical ion (positive or negative). ▶ Kinetic plots of ion-molecule reactions can be used to detect radical rearrangement.

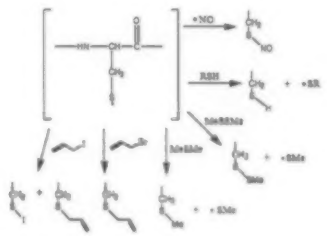

140–146

Comparison of collision-induced dissociation and electron-induced dissociation of singly charged mononucleotides

Viet Hung Nguyen, Carlos Afonso, Jean-Claude Tabet

▶ Sugar cross-ring cleavages are reinforced with EID. ▶ EID fragments can be representative of intra molecular non-covalent bonds. ▶ EID specific product ions are produced consecutively to the loss of H. ▶ H/D exchange and MS^3 experiments allowed explaining the dissociation pathways.

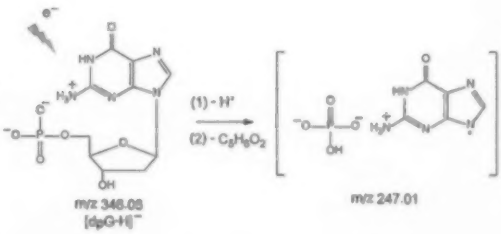

147–163

Gas phase acidity of a cysteine residue in small oligopeptides

Jialin Shen, Jianhua Ren

► The gas-phase acidities of small cysteine-containing peptides showed large variation. ► Tripeptides were slightly more acidic than the corresponding dipeptides. ► The N-cysteine peptides were more acidic than the isomeric C-cysteine ones. ► The differences in the gas-phase acidities were largely due to conformational effects.

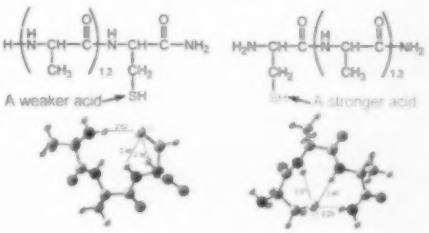

157–163

Chemical ionization in the atmosphere? A model study on negatively charged "exotic" ions generated from Titan's tholins by ultrahigh resolution MS and MS/MS

Árpád Somogyi, Mark A. Smith, Véronique Vuitton, Roland Thissen, István Komáromi

► A systematic FT-ICR and LTQ-Orbitrap ultrahigh resolution MS and MS/MS study is presented. ► ESI and LDI generated negative ions from "tholin" samples were studied. ► The negative ions are highly unsaturated and contain cyano functionality. ► Structurally related species (families) were proposed. ► The current study may have relevance to Titan's atmospheric chemistry.

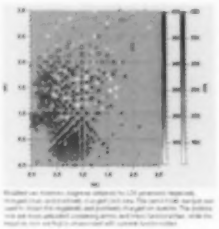

164–173

A systematic study on the effect of histidine position and fragment ion size on the formation of b_n ions

Mahsan Miladi, Behrooz Zekavat, Sharon M. Munisamy, Touradj Solouki

► We examine the effect of His position and fragment size on b_4–b_7 ion structures. ► b_4–b_7 have two conformers with different H/D exchange reactivities. ► b_4–b_7 fragment ions exhibit two ion populations in H/D exchange reactions. ► The presence of two conformers for b_4–b_7 is independent of His position. ► IMS of b_5 from peptides with His in positions 3–5 show two ion populations.

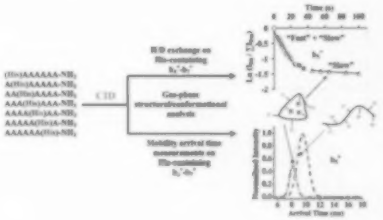

174–181

IRMPD spectroscopy b_2 ions from protonated tripeptides with 4-aminomethyl benzoic acid residues

Michael J. Kullman, Samuel Molesworth, Giel Berden, Jos Oomens, Michael Van Stipdonk

► Infrared multiple photon dissociation (IRMPD) spectroscopy and density functional theory (DFT) calculations used to study fragmentation of peptides that contain 4-aminomethylbenzoic acid residues. ► Dominant product ion from protonated AAG, A(AMBz)G and (AMBz)AG is b_2^+. ► IRMPD and DFT calculations suggest that the b_2 ion generated from A(AMBz)G has an acylium structure while b_2 ion from (AMBz)AG is instead a conventional oxazolone.

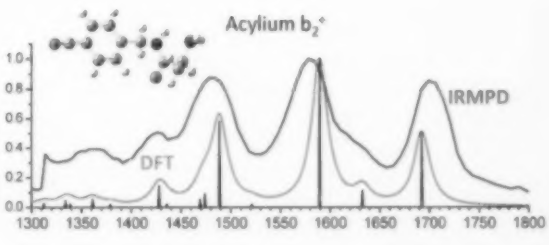

182–191

The simplest b_2^+ ion: Determining its structure from its energetics by a direct comparison of the threshold collision-induced dissociation of protonated oxazolone and diketopiperazine

P.B. Armentrout, Amy A. Clark

► The structure of the b_2^+ ions derived from protonated GGG and GAG are shown to be oxazolones by comparison of their energetics for decomposition with theoretical calculations. ► The energetics and fragmentations patterns of the b_2^+ ions differ appreciably from the isobaric protonated diketopiperazine species. ► Because the higher energy processes involve substantial kinetic energy release, it is shown that statistical analyses of these pathways does not provide useful thermodynamic information.

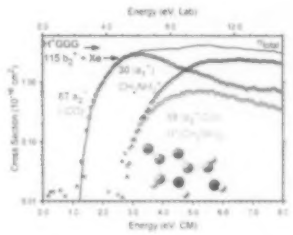

192–198

Kinetic and mechanistic studies of low-pressure ion–molecule association reactions of unsaturated Ru(II) complexes with CO

Ameneh Gholami, Travis D. Fridgen

► Chemically activated ion–molecule complexes. ► Radiative association. ► Ion–molecule association mechanism.

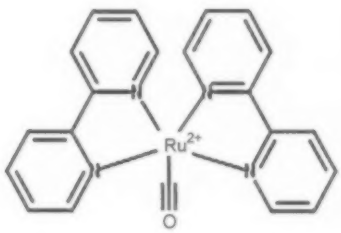

199–205

Fragmentations of protonated cyclic-glycylglycine and cyclic-alanylalanine

P.Y. Iris Shek, Justin Kai-Chi Lau, Junfang Zhao, Josipa Grzetic, Udo H. Verkerk, Jos Oomens, Alan C. Hopkinson, K.W. Michael Siu

► We used collision-induced dissociation method to study the fragmentation of protonated cyclic dipeptides. ► Distinctive fragment ions at low collision energies are observed from protonated cyclo-GG and cyclo-AA. ► Fragmentation mechanisms have been studied by density functional theory. ► Infrared multiple-photon dissociation has been used to characterize the fragment ion $[M+H-NH_3-CO]^+$ derived from protonated cyclo-AA.

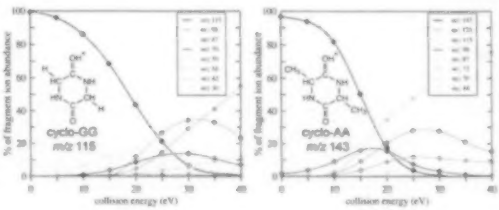

206–215

Site-specific hydrogen exchange and hydrogen transfer processes preceding the fragmentation of long-lived radical cations of ethyl dihydrocinnamate and related arylalkanoates

Aaron W. Amick, Edward Hoegg, Sean Harrison, Katelyn R. Houston, Richard R. Hark, I. David Reingold, Dieter Barth, Matthias C. Letzel, Dietmar Kuck

►Complete 4H-scrambling in metastable radical cations of ethyl dihydrocinnamate. ►Specific hydrogen transfer involving the benzylic methylene and *ortho*-positions. ► Hidden hydrogen exchange in ionised arylalkyl esters. ► Multistep fragmentation involving distonic ions and I/N complexes. ► Highly structure-specific fragmentation behaviour.

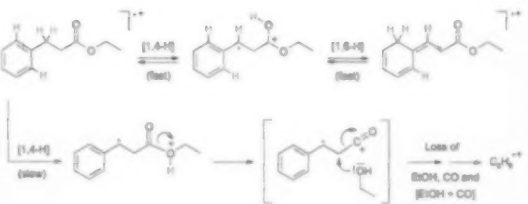

216–226

Structure of anionic *c*-type peptide fragments elucidated by IRMPD spectroscopy

Josipa Grzetic, Jos Oomens

► First IR spectra for anionic *c*-type peptide fragments. ► Comparison between experimental and DFT computed spectra suggests linear peptide structures with C-terminal amide group. ► Deprotonation sites identified: competition between peptide bond nitrogen atom and side chain depending on residue.

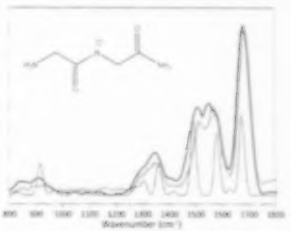

227–234

Tyrosine side-chain catalyzed proton transfer in the YG a_2 ion revealed by theory and IR spectroscopy in the 'fingerprint' and X—H (X = C, N, O) stretching regions

Benjamin J. Bythell, Oscar Hernandez, Vincent Steinmetz, Béla Paizs, Philippe Maître

► Structure and energetics of YG a_2 ion are investigated by MS/MS and theory. ► IRMPD spectroscopy is performed in the 'fingerprint' and X—H stretching regions. ► Infrared isomer-specific signatures of two isomers of YG a_2 ion are observed. ► 1,3-Proton transfer within a 5-membered ring is caralyzed by tyrosine side-chain.

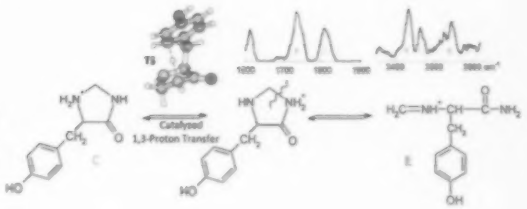

235–243

Ternary complexes of poly(ethylene imine), single-stranded oligodeoxynucleotides and glutamic acid moieties

Danijela Smiljanic, Chrys Wesdemiotis

► Molecular self-assembly to non-covalent ternary complexes (terplexes). ► The major self-assembly products have a stoichiometry of 1:1:1. ► Longer glutamic acid n-mers decrease the terplex stabilities. ► Solution and intrinsic stabilities of the terplexes follow the same order. ► Terplex stability is sensitive to nucleotide sequence if the Glu n-mer is short.

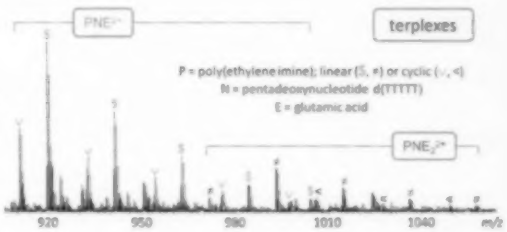

244–250

Resolving the α-effect in gas phase S_N2 reactions: A Marcus theory approach

John M. Garver, Zhibo Yang, Charles M. Nichols, Benjamin B. Worker, Scott Gronert, Veronica M. Bierbaum

► Experimental and theoretical studies on the α-effect in gas-phase S_N2 reactions. ► Using Marcus theory to provide insight into the intrinsic nature of the α-effect. ► Defining "normal" reactivity is a key in assessing the magnitude of the α-effect. ► Significantly lower electron affinities are associated with the formation of the α-oxyanions compared to the normal oxyanions. ► Differential solvation plays a dominant role in the magnitude of the α-effect in solution.

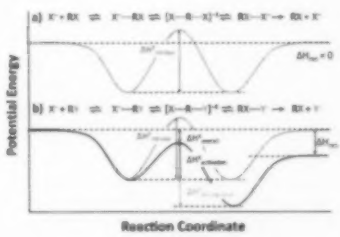

251–258

Energy and entropy effects in dissociation of peptide radical anions

Julia Laskin, Zhibo Yang, Corey Lam, Ivan K. Chu

► We studied the effect of the charge, radical, and basic residue on the energetics and dynamics of dissociation of peptide ions. ► We used surface-induced dissociation combined with RRKM modeling. ► Even-electron ions are more stable toward fragmentation than their odd-electron counterparts. ► Fragmentation of radical anions is entropically favored. ► Single population of structures adequately describes the observed kinetics of fragmentation.

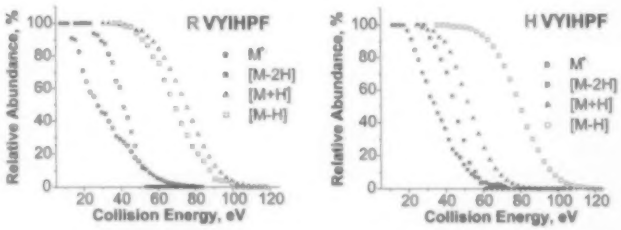

259–267

Influence of a gamma amino acid on the structures and reactivity of peptide a_3 ions

Matthew C. Bernier, Bela Paizs, Vicki H. Wysocki

► CID of protonated AGabaAlG leads to an unusually abundant a_3 ion. ► The AGabaA b_3 ion undergoes head-to-tail cyclization while AAA does not. ► Barriers to the $a_3 \rightarrow b_2$ and $a_3 \rightarrow a_3^*$ reactions are significantly higher for the AGabaA sequence than for AAA. ► The AGabaA a_3 ion undergoes head-to-tail cyclization while the AAA does not.

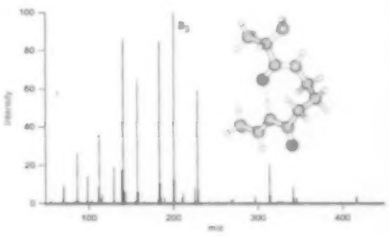

268–272

Elimination of water from the backbone of protonated tetraglycine

Justin Kai-Chi Lau, Junfang Zhao, K.W. Michael Siu, Alan C. Hopkinson

► DFT has been applied to study the mechanism for the elimination of water from $[G_4+H]^+$. ► The b_4 ion from $[G_4+H]^+$ is N_1-protonated 3,5-4*H*-imidazol-4-one. ► Formation of b_4 oxazolone from $[G_4+H]^+$ has identical barrier but thermodynamically less favourable. ► Formation of oxazole from $[G_4+H]^+$ is not competitive to the other pathways.

273–283

Proton and potassium affinities of aliphatic and N-methylated aliphatic α-amino acids: Effect of alkyl chain length on relative stabilities of K^+ bound zwitterionic complexes

Y. Tsang, Catherine C.L. Wong, Carrie H.S. Wong, Jackie M.K. Cheng, N.L. Ma, C.W. Tsang

► ZW1/CS1 K^+ affinities and proton affinities linearly correlated ($r^2 \geq 0.95$). ► For ZW1, greater deformation energy, E_{def}, found for smaller glycine/alanine. ► ZW1 K^+ affinities for Val, Leu and Ile found within a narrow 2 kJ mol^{-1} range. ► Leveling off of molecular polarizability contributions in Val, Leu and Ile. ► Similar ZW1/CS1 K^+ affinity trends in N-methylated aliphatic amino acids.

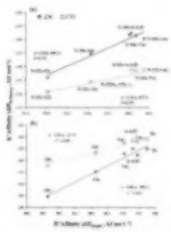

284–291

The influence of a C-terminal basic residue on peptide fragmentation pathways

Ross Chawner, Claire E. Eyers, Simon J. Gaskell

► Removal of a C-terminal basic residue generates peptides with substantially different fragmentation properties by MS/MS. ► Changes in fragmentation properties are attributed to a consequent effect upon the propensity to retain charge and stability of fragment ions. ► The observed dominant ion series from both CID and ETD is at least in part determined by the site of highest gas phase basicity. ► The data suggest a complementary value in proteome analyses for MS/MS of tryptic/Lys-C peptides with and without carboxypeptidase B treatment.

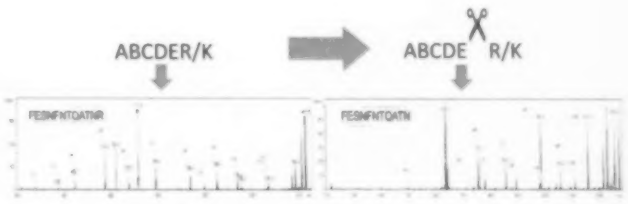

292–299

Fragmentation of protonated dansyl-labeled amines for structural analysis of amine-containing metabolites

Jiamin Zheng, Liang Li
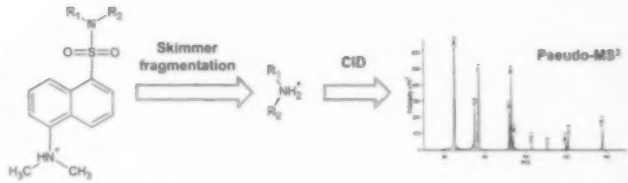
► MS/MS and MS^3 spectra of dansylated amines do not give much structural information. ► Skimmer-fragmentation can produce ions with *m/z* corresponding to the protonated unlabeled amines. ► MS/MS of the ions generates similar fragment ions as those of MS/MS of protonated unlabeled amines. ► These pseudo-MS^3 spectra can be used for identification of dansylated amines.